

# PROCEEDINGS

## 2008 EUMETSAT Meteorological Satellite Conference

Darmstadt, Germany, 08 -12 September 2008

### **Scientific Programme Committee:**

Peter Bauer (ECMWF)  
Hans Bonekamp (EUMETSAT)  
Heinrich Bovensmann (Universität Bremen)  
Lars Anders Breivik (DMI Norway)  
John Eyre (Met Office)  
Volker Gärtner (EUMETSAT)  
Jochen Grandell (EUMETSAT)  
Kenneth Holmlund (EUMETSAT)  
Marianne König (EUMETSAT)  
Vincenzo Levizzani (CNR)  
Rosemary Munro (EUMETSAT)  
Vesa Nietosvaara (FMI)  
Thierry Phulpin (CNES)  
Peter Schlüssel (EUMETSAT)  
Lothar Schüller (EUMETSAT)  
Jörg Schulz (DWD)  
Roger Saunders (Met Office)  
Piotr Struzik (Polish Met Service)  
Pedro Viterbo (IM Portugal)  
Xiangquian Wu (NOAA)

### **Conference Organising Committee:**

Madeleine Pooley, EUMETSAT  
Gabriele Kermann, EUMETSAT

Published and distributed by:

EUMETSAT  
Am Kavalleriesand 31  
64295 Darmstadt  
Germany

EUM P.52  
ISBN 978-92-9110-082-8  
ISSN 1023-0416  
Meteorological Conferences

Copyright ©EUMETSAT 2008.

This copyright notice applies only to the overall collection of papers: authors retain their individual rights and should be contacted directly for permission to use their material separately. Contact EUMETSAT for permission pertaining to the overall volume. The papers on this CD comprise the proceedings of the Conference mentioned on the label. They reflect the authors' opinions and are published as presented, without editing. Their inclusion in this publication does not necessarily constitute endorsement by EUMETSAT or the co-organisers.

# AN ANGULAR AND EMISSIVITY DEPENDENT ALGORITHM TO DETERMINE SEA SURFACE TEMPERATURE FROM MSG-SEVIRI DATA

Raquel Niclòs, Maria J. Estrela, Jose A. Valiente, and Maria J. Barberà

Fundación Centro de Estudios Ambientales del Mediterráneo – CEAM, 14 Charles Darwin, 46980 Paterna, Spain, niclos@ceam.es

## Abstract

A frequent and high-accuracy determination of Sea Surface Temperature (SST) would permit an improvement in the forecasting of natural hazards and the monitoring of the effects of climate change. The Spinning Enhanced Visible and Infrared Imager (SEVIRI) on board the geostationary METEOSAT Second Generation (MSG) platforms offers this possibility. Algorithms for SST retrieval from MSG-SEVIRI data have angular dependent coefficients to consider the high variability of the satellite zenith angle within an image, but do not use Sea Surface Emissivity (SSE) as an input. Nevertheless, SSE depends on the observation angle and surface wind speed, and its variability within a satellite image is similar to the emissivity variation for land surfaces, for which algorithms do include emissivity-dependent terms. An angular and emissivity dependent split-window equation is here proposed with the aim of determining SST to a reasonable level of accuracy for any observation angle. This equation was previously developed for the MODIS on the polar-orbiting EOS Terra/Aqua satellites (Niclòs et al. 2007), for which satisfactory validation results were obtained by comparison with in situ data. The equations for both SEVIRI sensors on board MSG1 and MSG2 platforms are provided in the current work, together with the first validation results.

## INTRODUCTION

Although Sea Surface Temperature is accurately determined from satellite observations as compared with other geophysical magnitudes, the requirements for higher accuracies are constant for applications in climate monitoring and operational oceanography. A high SST accuracy is achieved using the current split-window equations at nadir satellite viewings. However, SST uncertainties usually increase with the observation angle, and the retrieved SST does not seem to be accurate enough for observation angles larger than 40-50° (Niclòs et al. 2007). Some of the current sensors on polar-orbiting satellites have wide swaths in the across-track direction (e.g., the MODIS on EOS Terra/Aqua platforms or the AVHRR/3 on NOAA 17/18 and MetOp-A), with large observation angles near the image edges. The problem is even worse for radiometers on board geostationary satellites, such as the Spinning Enhanced Visible and Infrared Imager (SEVIRI) on board Meteosat Second Generation (MSG), since high-latitude regions are always observed at large observation angles. Figure 1 shows the observation angles within MSG-SEVIRI imagery. Extensive areas (such as all Europe) are observed at angles larger than 40°. Although angular and SST tendencies on the residual errors for MSG-SEVIRI data cannot be easily distinguished, since these variables are related to latitude for geostationary systems, SST errors have been proved to increase with observation angle when using current split-window algorithms on data collected from polar-orbiting platforms (e.g., for EOS-MODIS (Niclòs et al. 2007)).

SST determination from satellite TIR data requires atmospheric and emissivity corrections. Angular effects on these corrections have to be properly dealt with to avoid increases in SST uncertainty with angle. Besides an increase in the atmospheric path, Sea Surface Emissivity (SSE) shows a significant decrease at large viewing angles in relation to the nadir value. For instance, an SSE reduction of about 5 % at 11  $\mu\text{m}$  and of 7% at 12  $\mu\text{m}$  can be observed from 0° to 65°, and not considering the SSE decrease can cause high SST systematic errors. Figure 2 shows the SSE angular variation for MSG-

SEVIRI channels 9 and 10 (at about 11  $\mu\text{m}$  and 12  $\mu\text{m}$ , respectively) for two values of surface wind speed,  $U$ . SSE values of 0.992 and 0.989 are obtained for channels 9 and 10 at nadir, whereas values of 0.941 and 0.919 are determined for  $U = 0 \text{ m s}^{-1}$  at  $65^\circ$  (Wu and Smith 1997).

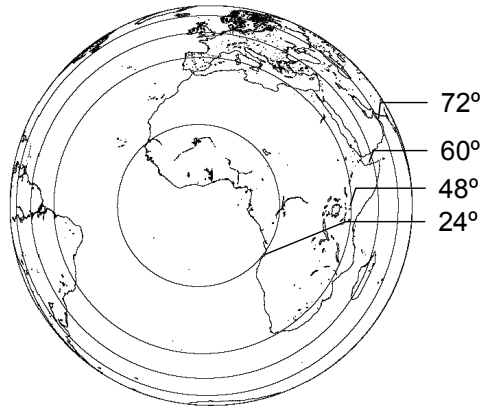


**Figure 1:** Satellite zenith angle within MSG-SEVIRI imagery (Merchant et al. 2006). Extensive areas of a SEVIRI image (such as the whole of Europe) are always observed at large angles ( $> 40^\circ$ ).

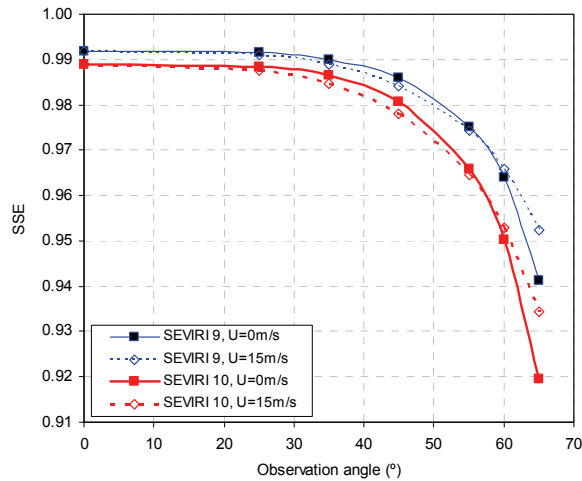


**Figure 2:** SSE angular variation for MSG-SEVIRI channels 9 and 10 and wind speeds of  $0 \text{ m s}^{-1}$  and  $15 \text{ m s}^{-1}$ .

Consequently, the range of SSE variability within an image due to the angular and wind speed dependences can be comparable to the variation shown by other natural emitting surfaces, such as soils and vegetation, at nadir. Therefore, we considered appropriate the introduction of an explicit dependence on the SSE in an SST split-window algorithm, similar to that proposed by Coll and Caselles (1997) for land surface temperature estimates. The use of emissivity terms is widely extended for land surface temperature retrievals. However, the inclusion of explicit SSE terms is not common in the current operational SST algorithm, e.g. for MODIS (Brown and Minnet 1999), AVHRR (Walton et al. 1998), SEVIRI (O&SI SAF Project Team 2006) and (A)ATSR (Zavody et al. 1995). We previously developed an emissivity dependent split-window equation for the MODIS (Nicolòs et al. 2007). The comparison between the SSTs estimated by the proposed equation and the concurrent in situ data collected by buoys (after a bulk-skin temperature difference correction) showed an algorithm accuracy of about  $\pm 0.3\text{K}$  for any observation angle. Emissivity dependent equations for both SEVIRI sensors on board MSG1 and MSG2 platforms are developed in the following section.

## ALGORITHM DEVELOPMENT

The proposed equation follows the model of Coll and Caselles (1997), which incorporates separate terms for the atmospheric and emissivity corrections. This split-window model can be written as:

$$T = T_i + a (T_i - T_j) + b (T_i - T_j)^2 + c + B(\epsilon) \quad (1)$$

where  $T$  is the surface temperature, and  $T_i$  and  $T_j$  are the brightness temperatures in the split-window channels, i.e., bands 9 and 10 of MSG-SEVIRI (9.8-11.8 $\mu$ m and 11– 13 $\mu$ m, respectively).  $a$ ,  $b$  and  $c$  are the atmospheric coefficients, which are independent of the surface properties (Coll and Caselles, 1997). The split-window technique takes advantage of the different absorption between the two split-window bands, which is closely correlated with atmospheric conditions, mainly the water vapour and air temperature profiles. Equation (1) assumes a quadratic dependence on the brightness temperature difference  $T_i-T_j$ , since the original linear function showed dependence on the atmospheric conditions and a quadratic function was considered better as a global algorithm.

Emissivity effects are compensated by the term  $B(\epsilon)$ . This term depends on the average SSE,  $\epsilon=(\epsilon_i+\epsilon_j)/2$ , and the SSE difference,  $\Delta\epsilon=\epsilon_i-\epsilon_j$ , for both split-window channels, as follows:

$$B(\epsilon)=\alpha(1-\epsilon)-\beta\Delta\epsilon \quad (2)$$

where  $\alpha$  and  $\beta$  depend both on the atmospheric properties, so as to characterise the reflection of the downwelling sky radiance, and on the surface temperature (Coll and Caselles, 1997).

The study of the dependences of all these terms and the assessment of coefficients for the SST retrieval from MSG-SEVIRI data was carried out by using synthetic data generated from atmospheric profiles and the radiative transfer code MODTRAN 4 (Berk et al. 1999). A set of 402 cloud-free atmospheric profiles selected by François et al. (2002) was used to generate the simulation database. The generation of the training database consisted of simulating top-of-atmosphere brightness temperatures for each radiometer channel when each of the atmospheric profiles is assumed. Atmospheric upwelling and downwelling radiances and transmittances were simulated by introducing the SAFREE profiles in the radiative transfer code MODTRAN 4. SSE values were calculated by using the model of Wu and Smith (1997), which accurately reproduces the effective SSEs for any wind speed and observation angle, even for angles larger than 50° (Nicolòs et al. 2005). Four values of surface wind speed were used: 0, 5, 10 and 15 m/s.  $T_9$  and  $T_{10}$  were obtained for each of the 402 SAFREE atmospheric profiles, assigning three SST values for each radiosounding:  $T_0$ ,  $T_0 - 3$  K and  $T_0 + 3$  K,  $T_0$  being the temperature of the first level at 1000 hPa. Additionally, in order to develop an angular-dependent split-window algorithm, seven at-surface observation angles were considered. Consequently, 33,768 simulation cases were computed (402 atmospheric profiles  $\times$  7 observation angles  $\times$  4 wind speeds  $\times$  3 SST values). Each simulation case consisted of a set of SST,  $T_9$ ,  $T_{10}$ ,  $\epsilon_9$ ,  $\epsilon_{10}$ , and  $W_0$ , i.e., the data required to be fitted to an equation like (1).

Atmospheric surface-independent coefficients ( $a$ ,  $b$ , and  $c$  of eq.(1)) were calculated for MSG-SEVIRI by means of a regression analysis between SST- $T_9$  and  $T_9-T_{10}$ , where the top-of-atmosphere brightness temperatures are obtained by considering the surface as a black-body ( $\epsilon = 1$  and  $\Delta\epsilon = 0$ ). For a given observation angle, the different atmospheric absorption produced by the water vapour content of the diverse profiles is the major cause of the temperature differences SST- $T_9$  and  $T_9-T_{10}$ . Nevertheless, the atmospheric correction required for a given atmospheric profile increases with the observation angle,  $\theta$ , as a consequence of the atmospheric path enlargement (i.e., the optical path increases by a factor  $\sec(\theta)-1$ ). Taking into account the higher increase in SST- $T_9$  than in  $T_9-T_{10}$  with angle, an angular dependence of the atmospheric coefficients is required to fit these differences at any angle. Figure 3 shows the fitting functions for several observation angles. The obtained fitting parameters show that atmospheric coefficients can be expressed as a linear function of  $\sec(\theta)-1$ . Similar coefficient expressions were suggested by François et al. (2002) for a global algorithm, but without considering an additional emissivity correction term.

Once the atmospheric correction coefficients have been estimated, the effect of the SSE can be compensated by means of the term  $B(\epsilon)$  (eq.(2)). The expressions for the coefficients of this term were adapted from the relationships given by Coll and Caselles (1997), changing the assumption of Lambertian reflection for land surfaces to specular reflection for sea surfaces (Nicolòs et al. 2007). Since coefficients  $\alpha$  and  $\beta$  depend on the atmospheric properties, they should depend on the column water vapour content and the observation angle, with the dependence on the observation angle being approximately negligible compared with the water vapour dependence, which was considered as a function of the oblique column water vapour content,  $W$ , defined as  $W=W_0/\cos(\theta)$ . Quadratic functions

were obtained from regression analyses of  $\alpha$  and  $\beta$  against  $W$ :  $\alpha = \alpha_0 + \alpha_1 W + \alpha_2 W^2$  and  $\beta = \beta_0 + \beta_1 W + \beta_2 W^2$ . Figure 4 shows these dependences for the MSG-SEVIRI simulated data, when all the observation angles are considered. Coefficients of determination,  $r^2$ , and fit standard errors,  $\sigma$ , of  $r_\alpha^2 = 0.90$ ,  $r_\beta^2 = 0.91$ ,  $\sigma_\alpha = \pm 3K$  and  $\sigma_\beta = \pm 8K$  were obtained by regression. Part of the dispersion shown in this figure could be a consequence of not considering the angular dependence. However, their effect in terms of temperature, through the term  $B(\varepsilon)$ , is low (with RMSE lower than  $\pm 0.15 K$ ).

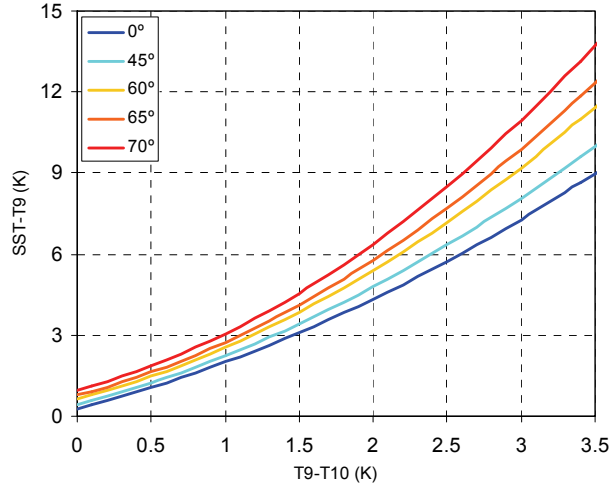


**Figure 3: Fitting functions between SST-T<sub>9</sub> and T<sub>9</sub>-T<sub>10</sub> for several observation angles.**

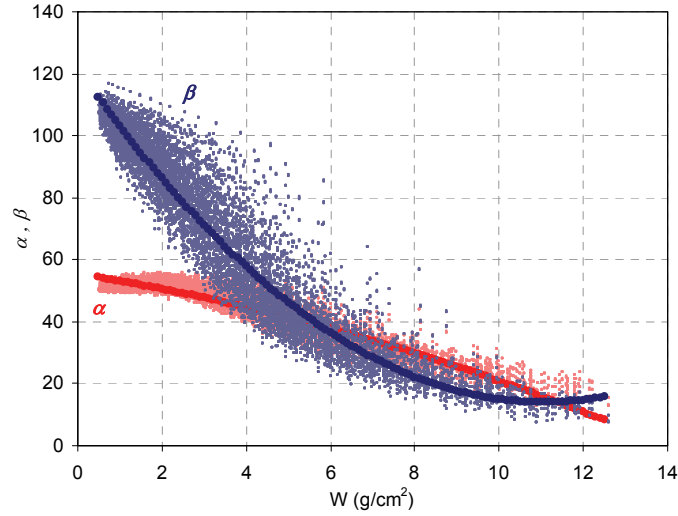


**Figure 4: Regression of the coefficients  $\alpha$  and  $\beta$  against the oblique column water vapour content,  $W = W_0 / \cos(\theta)$ , for the MSG-SEVIRI simulations obtained at any angle.**

Finally, we propose the following equation to deal with the atmospheric and emissivity corrections:

$$SST = T_9 + (a_1 S + a_2)(T_9 - T_{10}) + (b_1 S + b_2)(T_9 - T_{10})^2 + (c_1 S + c_2) + (\alpha_0 + \alpha_1 W + \alpha_2 W^2)(1 - \varepsilon) - (\beta_0 + \beta_1 W + \beta_2 W^2)\Delta\varepsilon \quad (3)$$

Atmospheric and emissivity correction coefficients of eq.(3) are given in Tables 1 and 2, respectively, for the SEVIRIs on MSG-1 and MSG-2.

SEVIRI	$a_1$	$a_2$	$b_1$	$b_2$	$c_1$	$c_2$
MSG-1	0.00±0.02	1.434±0.015	0.171±0.006	0.301±0.005	0.373±0.014	0.269±0.005
MSG-2	-0.04±0.02	1.237±0.015	0.153±0.005	0.271±0.004	0.352±0.015	0.249±0.005

**Table 1: Atmospheric correction coefficients of eq.(3) for the SEVIRI sensors on MSG-1 and MSG-2.**

SEVIRI	$\alpha_0$	$\alpha_1$	$\alpha_2$	$\beta_0$	$\beta_1$	$\beta_2$
MSG-1	55.34±0.05	-2.18±0.02	-0.127±0.002	121.79±0.15	-19.52±0.07	0.883±0.007
MSG-2	56.17±0.05	-2.49±0.02	-0.106±0.002	109.07±0.13	-17.09±0.06	0.758±0.006

**Table 2: Emissivity correction coefficients of eq.(3) for the SEVIRI sensors on MSG-1 and MSG-2.**

## DETERMINATION OF INPUT VARIABLES

### Sea surface emissivity

The SSE values required in eq.(3) can be obtained using the model of Wu and Smith (1997). Niclòs et al. (2005) compared the models for the SSE determination given in the bibliography with experimental data, and concluded that the model of Wu and Smith (1997) was the most accurate for any observation angle and wind speed. This model is a physical characterization of the sea surface emission, including the reflected emission, but it is mathematically quite complex. For this reason, we developed a simple parametrization to calculate SSEs as a function of the surface wind speed,  $U$ , and the observation angle,  $\theta$  (Niclòs and Caselles 2005):

$$\varepsilon_k(\theta, U) = \varepsilon_k(0^\circ) [\cos(\theta^{(cU+d)})]^{b_k} \quad (4)$$

This simple equation permits the determination of SSE for a sensor channel  $k$ ,  $\varepsilon_k(\theta, U)$ , from its value at nadir,  $\varepsilon_k(0^\circ)$ , using only three coefficients:  $c = -0.037 \pm 0.003$  s/m,  $d = 2.36 \pm 0.03$ , and  $b_k$ , the last being dependent on the channel.  $\varepsilon_k(\theta, U)$  and  $b_k$  values are given in Table 3 for both SEVIRIs.

SEVIRI	$\varepsilon_9(0^\circ)$	$\varepsilon_{10}(0^\circ)$	$b_9$	$b_{10}$
MSG-1	0.99176±0.00003	0.98875±0.00005	0.0347±0.0015	0.0483±0.0018
MSG-2	0.99172±0.00003	0.98835±0.00005	0.0347±0.0015	0.0494±0.0019

**Table 3: Emissivities at nadir and  $b_k$  coefficients of equation (4) for MSG-1 and MSG-2 SEVIRI channels 9 and 10.**

The effect of surface wind speed is especially important for observation angles of over 55-60° (Wu and Smith 1997, see also Figure 2), and consequently the use of this parametrization with wind satellite imagery could improve the SSE estimates, and thus SST retrievals, for such angles.

### Water vapour content

There are different methods for estimating the oblique water vapour content,  $W$ , required in equation (3), e.g., by taking advantage of solar radiance attenuation by water vapour in the near-infrared region or by integrating the humidity atmospheric profiles. However, SEVIRI does not have the required channels for the determination of water vapour content using these methods, and  $W$  retrieval from SEVIRI data involves combinations of mid-infrared and thermal-infrared channels. The soundness of the currently existing methods was checked using the generated simulation database. The SAFNWC Project Team (2007) proposed a methodology to estimate  $W_0$  over marine surfaces using SST,  $T_9-T_{10}$ ,  $\theta$ , and an atmospheric effective temperature as input magnitudes. However, the assumption of an SSE equal to 1 in its development and the requirement of SST as an input are weak points for this methodology. The fitting of the SAFNWC equation to the simulation data showed a poor correlation and an estimation error of  $\pm 0.8$  cm for  $W_0$ . The maximum  $W_0$  error required in order to obtain the SST with an accuracy higher than half a degree Kelvin by using equation (3) is approximately  $\pm 0.5$  cm, or  $\pm 0.9$  cm in terms of  $W$ . The SAFNWC method exceeds this maximum error. Sobrino et al. (2002) also proposed a simple equation for  $W_0$  retrievals over marine surfaces, but this again assumes blackbody behaviour for the sea, requires a previous estimate of atmospheric temperature and SST, and yields large estimation errors. The covariance-variance technique (Kleespies and Mc Millin, 1990) takes advantage of the radiance variability within a set of neighbouring pixels for which the atmosphere is homogeneous. This methodology can be applied to the SEVIRI bands, does not require assuming an SSE equal to 1 and shows a  $W_0$  estimation error of  $\pm 0.2$ cm. However, the low spatial variability of the SST and the sensitivity of the method to the radiometric noise of the instrument cause high inaccuracies when it is applied to SEVIRI images.

The water vapour content can also be retrieved by experimental regressions of  $W$  against brightness temperatures in several SEVIRI channels. We suggest the combination of bands 6, 7, 9, 10, and 11 following the angular equation:

$$W = k_6(\theta)T_6 + k_7(\theta)T_7 + k_9(\theta)T_9 + k_{10}(\theta)T_{10} + k_{11}(\theta)T_{11} + k_0(\theta) \quad (5)$$

where  $k_i(\theta) = k_{i,0} + k_{i,1}(S+1)$ ,  $S+1$  being equal to  $\sec(\theta)$ . Table 4 shows the coefficients of eq. (5).

	$K_{6,0}$	$K_{6,1}$	$K_{7,0}$	$K_{7,1}$	$K_{9,0}$	$K_{9,1}$
MSG-1	0.00±0.01	-0.087±0.005	-0.15±0.04	0.28±0.02	0.92±0.09	0.22±0.05
MSG-2	0.00±0.01	-0.086±0.005	-0.14±0.04	0.27±0.02	0.81±0.09	0.20±0.05
	$K_{10,0}$	$K_{10,1}$	$K_{11,0}$	$K_{11,1}$	$K_{0,0}$	$K_{0,1}$
MSG-1	-1.19±0.06	-0.43±0.03	0.425±0.014	0.167±0.08	2.87±0.16	-37.2±0.7
MSG-2	-1.08±0.06	-0.41±0.03	0.415±0.013	0.167±0.08	2.47±0.15	-36.5±0.7

**Table 4: Water vapour content coefficients of eq.(5).**

The fitting of equation (5) to the simulation data shows the best correlation ( $r^2=0.9$ ) and a  $W$  estimation error lower than  $\pm 0.8$ cm. Consequently, equation (5) provides a suitable method to obtain the water vapour content from SEVIRI data with the accuracy required for SST retrieval using equation (3). Equation (5) was also validated against concurrent sun photometer  $W$  measurements from the AERONET database (aeronet.gsfc.nasa.gov). Table 5 summarizes the validation results.

	$W(eq.5) - W_{in\ situ}$	$W_0 - W_{0\ in\ situ}$
<i>Bias</i> ( $cm^{-1}$ )	0.0	0.0
$\sigma$ ( $cm^{-1}$ )	0.8	0.5
<i>RMSE</i> ( $cm^{-1}$ )	0.8	0.5
<i>N. events</i>	597	597

**Table 5: Validation results for eq.(5).  $W_0$  is the vertical column water vapour content:  $W_0 = W \cos(\theta)$ .**

## VALIDATION

A matchup database of in situ buoy measurements concurrent with MSG-SEVIRI imagery was used for the validation. We centred the area of study in Europe, since images are always acquired at large observation angles for this area. In situ data were obtained from the National Data Buoy Center (NDBC) of the NOAA (<http://www.ndbc.noaa.gov/>) and from the Oceanic Data Base of the Spanish Ministerio de Fomento (<http://www.puertos.es/>). In situ buoy SST data measured at night, or during the day when surface wind speed is  $\geq 6$  m/s, were considered here for validation, since in these cases a constant difference between skin and sub-surface temperatures exists and can be subtracted from buoy data to obtain values comparable to the satellite retrieved data (Niclos et al. 2007). Once the in situ data were gathered and filtered for such wind speed values, concurrent cloud-free MSG-SEVIRI data were selected. Finally, a total of 8219 matchups were used. Figure 5 shows the spatial distribution of this matchup database.

The soundness of equation (3) for the retrieval of SST from MSG-SEVIRI, together with eq.(4) and eq.(5) for SSE and  $W$  determinations respectively, was analyzed using the described validation database. The first column of Table 6 shows the corresponding validation results. Additionally, the operational O&SI SAF SST algorithms (O&SI SAF Project Team 2006) were also compared with the in situ data, by using day or/and night data according to the algorithm expression (since the  $3.9 \mu m$  channel is only used at night). Some of these algorithms were adjusted to provide sub-skin temperatures, and buoy data were directly used for their validation (without skin effect correction). All these algorithms are angular-dependent but they do not use SSE values as input. Table 6 also shows a summary of the validation results for these algorithms. Since histograms of SST differences between the results of each algorithm and in situ data show distributions comparable to the Gaussian probability distribution, with low skewness coefficient and kurtosis values around 3, the bias and standard deviations reported in Table 6 are meaningful for checking the algorithm validities.

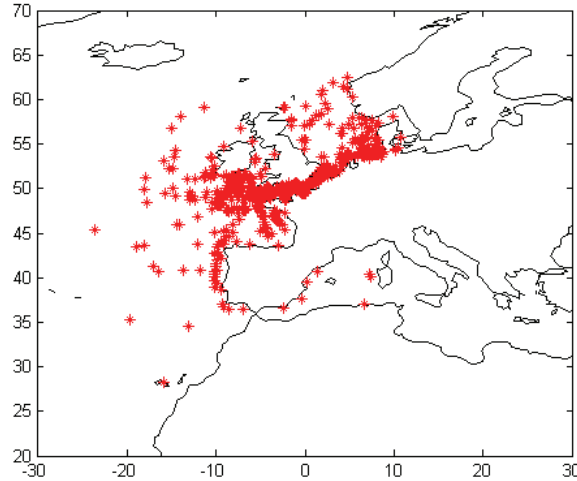


Figure 5: Distribution of the matchups used for the validation.

	SST <sub>algorithm</sub> – SST <sub>in situ</sub>			
	Proposed (eq.3)	O&SI SAF NLS*	O&SI SAF DGN*	O&SI SAF NGN*
Bias (K)	0.0	0.2	1.0	2
$\sigma$ (K)	0.5	0.6	0.9	1
RMSE (K)	<b>0.5</b>	<b>0.6</b>	<b>1.3</b>	<b>3</b>
Skewness	-0.06	-0.37	-0.19	-0.29
Kurtosis	2.89	3.60	3.00	3.47
P( $\pm 0.5K$ ) (%)	66	60	22	2
N. events	8219	8219	3226	3704

Table 6: Validation results for eq. (3) and the O&SI SAF SST algorithms (O&SI SAF Project Team 2006): Nonlinear (NLS), Day General (DGN) and Night General (NGN) algorithms. P( $\pm 0.5K$ )=proportion of SST differences within  $\pm 0.5$  K.

The proposed equation provides SSTs in good agreement with in situ data for observation angles from 40° to 70°, with negligible systematic errors and reasonably low standard deviations; its final accuracy is  $\pm 0.5K$ . The O&SI SAF non-linear algorithm (NLS), which requires a climatic SST as an input, shows a bias of 0.2K and a standard deviation of  $\pm 0.6K$ . However, the biases and standard deviations obtained for the O&SI SAF proposed general algorithms for day and night, DGN and NGN respectively, are much larger. The DGN and NGN algorithms use brightness temperatures at 8.7 $\mu m$  as inputs, and thus the low accuracies obtained for them,  $\pm 1.3K$  and  $\pm 3K$  respectively, could be related to the use of this SEVIRI channel.

## CONCLUSIONS

An angular-dependent split-window equation that incorporates an explicit dependence on Sea Surface Emissivity is proposed for SST retrieval, mainly from image areas observed at large viewing angles. The inclusion of such a term is not common in current operational SST algorithms. After the satisfactory results obtained using an emissivity-dependent equation for EOS Terra/Aqua - MODIS imagery (Nicolòs et al. 2007), this work provides an equivalent equation for the SEVIRI sensors on MSG-1 and MSG-2. The comparison between the SSTs estimated by the proposed equation (for observation angles from 40° to 70°) and the concurrent in situ data collected by buoys has shown an algorithm accuracy of  $\pm 0.5K$ . This accuracy is slightly better than the one determined for the O&SI SAF NLS algorithm when the same validation database is used, and much better than the values obtained by means of the O&SI SAF DGN and NGN algorithms for day and night, respectively (O&SI SAF, 2006). These results, together with those previously obtained for MODIS, point out the interest of using angular and emissivity dependent algorithms to retrieve SST for any observation angle.

## ACKNOWLEDGMENT

This work has been supported by the Spanish *Ministerio de Ciencia e Innovación* (projects CGL2005-03386, CGL2007-65774/CLI, and CONSOLIDER-INGENIO 2010 CSD2007-00067, as well as the Juan de la Cierva Research Contract of Dr. R. Niclòs, which is co-funded by the European Social Fund) and the European Union (Project CIRCE No. 036961). Fundació CEAM is supported by the Generalitat Valenciana and BANCAIXA.

## REFERENCES

- Berk, A., G.P. Anderson, P.K. Acharya, J. H. Chetwynd, L. S. Bernstein, E.P. Shettle, M.W. Matthew, and S.M. Adler-Golden, (1999) MODTRAN 4 user's manual. Air Force Research Laboratory, Space Vehicles Directorate, Air Force Materiel Command, Hascom AFB, MA, 95 pp.
- Brown, O. B., and P. J. Minnett, (1999) MODIS infrared sea surface temperature algorithm - Algorithm Theoretical Basis Document. Products: MOD28. ATBD Reference Number: ATBD-MOD-25.
- Coll C., and V. Caselles, (1997) A split-window algorithm for land surface temperature from advanced very high resolution radiometer data: Validation and algorithm comparison. *Journal of Geophysical Research*, **102(D14)**, pp 16697-16713.
- François, C., A. Brisson, P. LeBorgne, and A. Marsouin, (2002) Definition of a radio-sounding database for sea surface brightness temperature simulations: Applications to sea surface temperature retrieval algorithm determination. *Remote Sensing of Environment*, **81**, pp 309-326.
- Kleespies, T.J., and McMillin, L.M., (1990) Retrieval of precipitable water from observations in the split window over varying surface temperature. *Journal of Applied Meteorology*, **29**, pp 851-862.
- Merchant, C.J., Embury, O., Le Borgne, P., and Bellec, B., (2006) Saharan dust in nighttime thermal imagery: Detection and reduction of related biases in retrieved sea surface temperature. *Remote Sensing of Environment*, **104**, pp 15-30.
- Niclòs, R., E. Valor, V. Caselles, C. Coll, and J.M. Sánchez, (2005) In situ angular measurements of thermal infrared sea surface emissivity - Validation of models. *Remote Sensing of Environment*, **94(1)**, pp 83-93.
- Niclòs, R., and V. Caselles, (2005) Angular variation of the sea surface emissivity. *Recent Research Development in Thermal Remote Sensing*, Research Signpost, pp 37-65.
- Niclòs, R., V. Caselles, C. Coll, and E. Valor, (2007) Determination of sea surface temperature at large observation angles using an angular and emissivity dependent split-window equation. *Remote Sensing of Environment*, **111**, pp 107-121.
- O&SI SAF Project Team, (2006) Atlantic SST Product Manual (v.1.6). EUMETSAT O&SI SAF, 49 pp.
- SAFNWC, (2007) Software user manual for the PGE06 of the SAFNWC/MSG. EUMETSAT SAFNWC, 21 pp.
- Sobrino, J.A., Jimenez, J.C., Raissouni, N., and Soria, G., (2002) A simplified method for estimating the total water vapour content over sea surface surfaces using NOAA-AVHRR Channels 4 and 5. *IEEE Transactions on Geoscience and Remote Sensing*, **40**, pp 357-361.
- Walton, C. C., W. G. Pichel, J. F. Sapper, and D. A. May, (1998) The development and operational application of nonlinear algorithms for the measurement of sea surface temperatures with the NOAA polar-orbiting environmental satellites. *Journal of Geophysical Research*, **103 (C12)**, pp 27999-28012.
- Wu, X., and W.L. Smith, (1997) Emissivity of rough sea surface for 8-13  $\mu\text{m}$ : modelling and verification. *Applied Optics*, **36**, pp 2609-2619.
- Zavody, A.M., C.T., Mutlow, and D.T., Llewellyn-Jones, (1995) A radiative transfer model for sea surface temperature retrieval for the along-track scanning radiometer. *Journal of Geophysical Research*, **100**, pp 937-952.